ECS Transactions, 28 (21) 65-70 (2010)
10.1149/1.3496020 ©The Electrochemical Society

Nitrogen Doped Carbon Nanotubes Based Non-Precious Metal Catalysts for Oxygen Reduction Reaction at Alkaline Fuel Cell Cathode

Zhu Chen[a], and Zhongwei Chen[a,*]

[a] Department of Chemical Engineering, Waterloo Institute of Nanotechnology, Waterloo Institute of Sustainable Energy, University of Waterloo, Waterloo, Ontario N2L 3G1, Canada, *zhwchen@cape.uwaterloo.ca

Alkaline fuel cell is a highly efficient and environmentally friendly energy conversion device showing great potential for sustainable development. However, to realize the commercialization of alkaline fuel cell, many obstacles must be overcome. The biggest challenge is perhaps to improve the oxygen reduction reaction (ORR) at the alkaline fuel cell cathode. Platinum based catalyst remained to be the most effective catalyst for ORR, but the scarcity and high cost prohibit large scale application in alkaline fuel cell. Nitrogen doped carbon materials have showed great potential for ORR, making these catalysts desirable replacements for platinum based catalysts. In this paper, nitrogen doped carbon nanotube exhibiting high ORR activity is presented. Through material characterizations, the various factors affecting the activity of nitrogen doped carbon nanotube are elaborated as well.

Introduction

Alkaline fuel cells (AFCs) are potential sustainable energy conversion device for transport, stationary, and portable applications, owing to the low emission and high conversion efficiency of the device (1, 2). Although AFCs display many desirable features, numerous obstacles must be overcome before the commercialization. Sluggish oxygen reduction reaction (ORR) kinetics at the cathode side of AFCs is one of the key factors limiting the performance of alkaline fuel cells and it greatly hinders the widespread commercialization. To date, the best ORR catalysts are Pt and Pt-based materials, but owing to the high cost and scarcity, large scale commercialization of fuel cells using Pt-based catalyst is not economically feasible. As a result, lowering the cost of ORR catalyst on the cathode of AFCs must be addressed which can be realized through reduction of Pt loading or complete removal of precious metal from the catalyst composition. Different classes of catalysts have been proposed, including transition metal alloys (3) and chalcogenides (4). These materials showed promising ORR activity for fuel cell applications, however their performance is still inferior compared to that of the Pt and Pt-based catalysts.

The emerging field of nanotechnology can bring upon improvements towards ORR catalysts. One type of nanomaterials is carbon nanotubes (CNTs) which have high electrical conductivity, large surface area, and easy modification of surface material properties (5, 6). The surface modification of CNTs by nitrogen has been showed to improve the activity of carbon nanotubes (7), however the ORR performance is poor

compared with Pt-based materials (8, 9). In the study carried out by Gong et al, nitrogen doped carbon nanotubes (NCNTs) synthesized by the pyrolysis of iron (II) phthalocyanine showed higher stability and ORR activity compared to commercial Pt/C catalyst (10). The transition metal – nitrogen groups (i.e. FeN_2 or FeN_4) (11, 12) or the surface nitrogen groups (i.e. pyridinic or quaternary) (9, 13) have been proposed to be the attributing factors of the ORR activity of nitrogen doped carbonaceous materials. In both cases, the emphasis was placed on the nitrogen contents, thus nitrogen content can be correlated with ORR performance of catalysts. As a result, it is hypothesized that different nitrogen content can lead to different ORR activity.

This report proposed the synthesis of NCNTs with different nitrogen content using different nitrogen precursors. NCNTs showing high ORR activity in alkaline conditions were synthesized using pyridine (Py-NCNTs) or ethylenediamine (EDA-NCNTs) as the nitrogen precursors and ferrocene as the metal catalyst. The NCNTs synthesis was carried out using a chemical vapor deposition (CVD) system under ambient pressure. The physicochemical characterizations were carried out with transmission electron microscopy, X-ray photoelectron spectroscopy and Raman spectroscopy. The electrochemical activity towards ORR was evaluated using rotating ring disc electrode voltammetry (RRDE).

Experimental Methods

NCNT synthesis

NCNTs were grown using an injection CVD technique, carried out in a single zone tube furnace. A precursor solution was prepared dissolving ferrocene (98%, Aldrich) in pyridine (99%, Caledon Laboratory Chemicals) or ethylenediamine (98%, EMD Chemicals) at 2.5 wt. %. The precursor solution was injected into the furnace using a syringe pump at a constant rate. Short quartz tubes (O.D 18 mm, length 10 mm) were placed in the middle of the furnace which was used as substrates for NCNTs growth. The synthesis was carried out at 800 °C for 1 h under ambient condition. After synthesis, air was let into the reaction atmosphere and the NCNTs were collected from the soot deposit on the inner wall of short quartz tubes. The collected NCNTs were washed in 0.5 M sulfuric acid for 5 h followed by drying in vacuum oven overnight.

Physiochemical Characterization

Scanning electron microscopy (LEO FESEM 1530, 20 eV) (SEM) was used to investigate the overall morphology of the NCNTs. Transmission electron microscopy (Philips, CM300) (TEM) was used to investigate the detail surface structure as well as graphitization of NCNTs walls. X-ray photoelectron spectroscopy (Thermal Scientific K-Alpha XPS spectrometer) (XPS) was used to examine the elemental composition of the NCNTs samples and the content of the different surface nitrogen groups. Energy dispersive X-ray spectroscopy (EDX) was used to evaluate the elemental composition of the NCNTs samples. Raman spectroscopy (Bruker FT-Raman spectrometer) was used to qualitatively evaluate the degree of surface defect of NCNTs.

Electrochemical Characterization

Electrocatalytic activity evaluation was carried out by rotating ring disc electrode (RRDE) voltammetry. The RRDE voltammetry uses a bipotentiostat and a rotation speed controller (Pine Research Instrument). The RRDE experiment was carried out by depositing catalyst ink onto the glassy carbon portion of the RRDE. The ink was prepared by suspending 2 mg of catalyst in 1 mL of 0.2 wt. % nafion solution. The ink was sonicated until homogeneous suspension is achieved and 20 µL of ink was deposited onto the electrode and dried. Visual inspection was carried out to ensure uniform film formation and no ink deposition on the platinum ring. After the electrode preparation, RRDE voltammetry was carried out in 0.1 M KOH solution where the disc potential was varied from 0.2 to -1.2 V vs. Ag/AgCl (figures only show to 0.5 V) at a scan rate of 10 mV/s and the ring potential was held at 0.5 V. The electrolyte solution was saturated in N_2 gas for 30 min and the background signal was collected. After which, the experiment was carried out in oxygen saturated electrolyte.

Results and Discussion

TEM Analysis

From the TEM images showed in Figure 1, bamboo-like structure was observed for both EDA-NCNTs and Py-NCNTs. The bamboo-like structure is commonly observed for NCNTs (14-17) and it can be attributed to the formation of pentagon structures due to the incorporation of nitrogen atoms (18). Differences with respect to the diameter of the NCNTs and shape of the compartments can be seen. The EDA-NCNTs showed a slight reduction in diameter and more rounded compartment, whereas Py-NCNTs display larger diameter and more rectangular compartments. It should be noted that the reduction in diameter of the more nitrogen rich NCNTs has been observed, as documented by Terrones et al (14, 15).

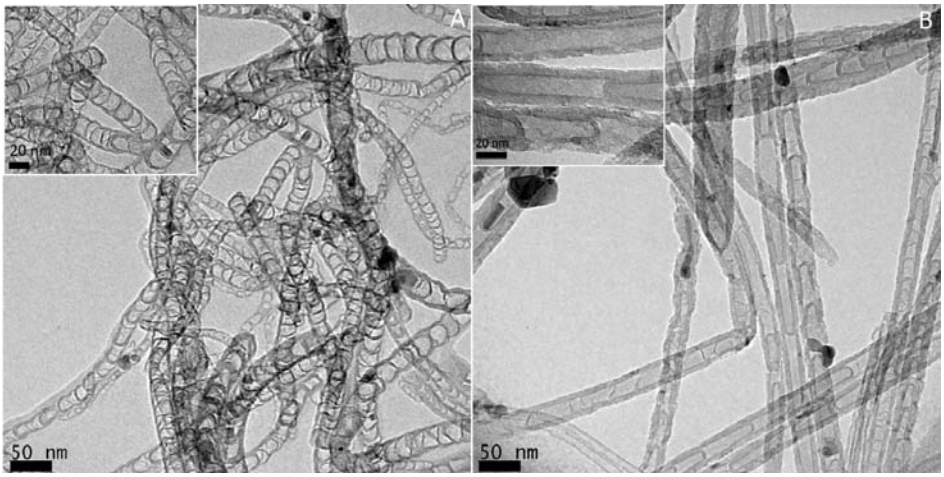

Figure 1. TEM image of A) EDA-NCNTs and B) Py-NCNTs.

XPS Analysis

The elemental composition of the NCNTs samples and different surface nitrogen group composition were investigated using XPS. The overall nitrogen content for EDA-NCNTs and Py-NCNTs is 4.74 at. % and 2.35 at. %, respectively. This result can be caused by the higher nitrogen content in the molecular structure of ethylenediamine

compared with pyridine. Similar trend has been previously reported where a positive correlation between the number of nitrogen atom in the structure of nitrogen precursor and the nitrogen content of the NCNTs samples was confirmed (19).

High resolution N 1S spectrum of the EDA-NCNTs and Py-NCNTs samples is showed in Figure 2. The peak centered at 400.75 eV for Py-NCNTs and 401.05 eV for EDA-NCNTs is close to the peak of pyrrolic nitrogen group at 400.5 eV and the peak of quaternary nitrogen group at 401.3 eV. The quaternary nitrogen group can be found on the basal plane of graphitic network, and the pyrrolic nitrogen group having a pentagonal structure can be found at the curved surface in the NCNTs. Thus, it is possible that both pyrrolic and quaternary nitrogen groups are the contributing factors for this peak. Formation of pyridone nitrogen group can be caused by the oxygen that was introduced into the growth environment after synthesis has completed.

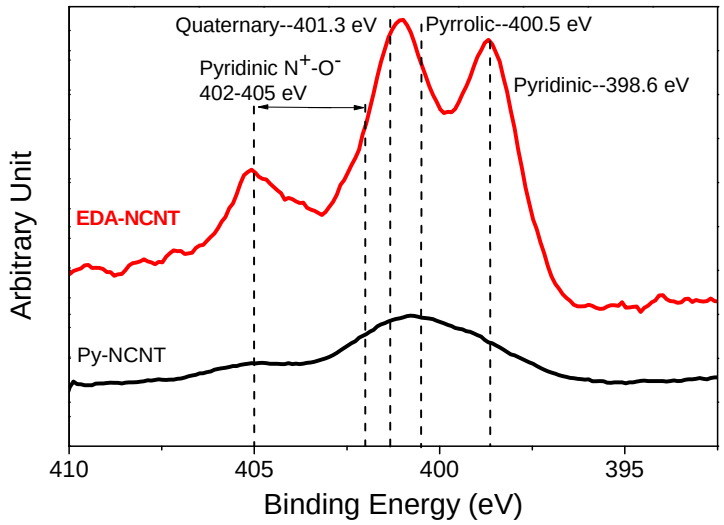

Figure 2. High resolution N 1S spectrum of EDA-NCNT and Py-NCNT showing the presence of different types of surface nitrogen groups.

Relative composition of the different surface nitrogen groups and their corresponding peak position are summarized in Table 1. It is evident that pyridinic nitrogen group is the dominant surface nitrogen group in EDA-NCNTs whereas quaternary nitrogen group is dominant in Py-NCNTs. This result agrees with previously reported literatures where NCNTs having higher overall nitrogen content tends to contain more pyridinic nitrogen groups (14, 20) and oppositely, for NCNTs contain lower overall nitrogen content, quaternary nitrogen groups is the dominant species (14, 15). Pyridinic nitrogen group has been attributed to be the active site for ORR due to the lone pair of electrons (21). Additionally, large amount of pyridinic nitrogen group that exists on the edge of graphite plane can be exposed by the surface defects observed in the NCNTs. The pyridinic content of EDA-NCNTs and Py-NCNTs is approximately 1.7 at. % and 0.3 at. % respectively which could suggest higher ORR activity for the EDA-NCNTs.

TABLE I. High resolution N1s signal showing the peak position and relative composition of different surface nitrogen groups.

	EDA-NCNTs		Py-NCNTs	
	Peak Position (eV)	At. %	Peak Position (eV)	At. %
Quaternary / Pyrrolic	401.05	45.91	400.75	68.20
Pyridinic	398.60	35.09	398.47	14.83
Pyridone	404.69	19.00	404.87	16.96

Polarization curve of ORR obtained from rotating ring disc electrode (RRDE) voltammetry is showed in Figure 3, and the important performance indicators of ORR catalysts is showed in Table 2. It is apparent that EDA-NCNTs is a much more superior catalyst compared to Py-NCNTs. EDA-NCNTs show three times limiting current density compared with Py-NCNTs indicating higher number of active site for ORR. The smaller onset and half wave potential of EDA-NCNTs also indicates a much faster kinetics for ORR compared with Py-NCNTs. With respect to the number of electrons transferred and H_2O selectivity, EDA-NCNTs showed a 12.6% and 21.6 % improvement respectively at -0.3 V. This indicates the more favourable four-electron pathway was the main ORR pathway for EDA-NCNTs, and the reduced H_2O_2 production. EDA-NCNTs was also compared with commercial Pt/C catalyst which showed slight improvement with respect to half wave potential, number of electrons transferred, and H_2O selectivity was observed.

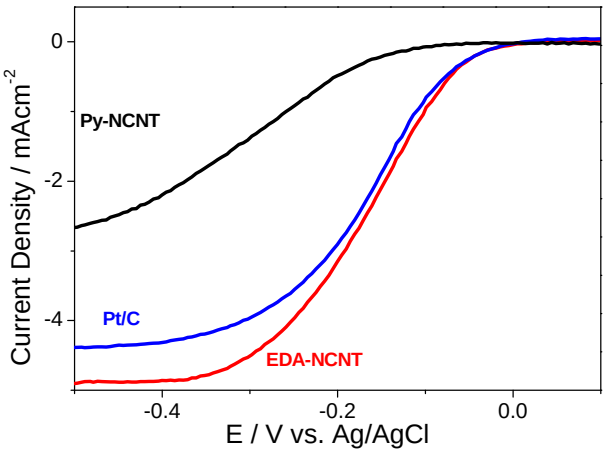

Figure 3. ORR polarization curve of EDA-NCNTs, Py-NCNTs and commercial Pt/C catalyst.

TABLE II. The important performance indicators of ORR catalysis. Starred (*) entries indicate values taken at -0.1 V and the double daggered entries (‡) indicates values taken at -0.3 V.

	Half Wave Potential (V)	Limiting Current Density ($mAcm^{-2}$, at 2500 rpm)	No. of Electrons Transferred (at 2500 rpm, -0.5 V)	H_2O Selectivity (%, at 2500 rpm, -0.5 V)
EDA-NCNTs	-0.15 V	-4.91	3.63^{*}	$3.85^{‡}$
Py-NCNTs	-0.33 V	-1.57	---	$3.42^{‡}$
Pt/C	-0.16 V	-4.39	3.55^{*}	$3.82^{‡}$

Active ORR catalysts based on NCNTs were synthesized using the same carbon precursor but different nitrogen precursors. Among the different catalysts, EDA-NCNTs were found to be much more superior to the Py-NCNTs. Based on the analysis, the nitrogen precursors were found to have direct effect on the overall nitrogen content of the NCNTs which in turn greatly influences the ORR activity of the catalyst. As a result, employing different nitrogen precursors can effectively tune the nitrogen content of the resultant NCNTs as well as the ORR activity.

Acknowledgments

This work was financially supported by the National Sciences and Engineering Research Council of Canada (NSERC) and the University of Waterloo.

References

1. L. Zhang, J. J. Zhang, D. P. Wilkinson, H. J. Wang, *J. Power Sources*, **156**, 171 (2006).
2. N. Limjeerajarus, T. Yanagimoto, T. Yamamoto, H. Ohashi, T. Ito, T. Yamaguchi , *J. Chem. Eng. Jpn.*, **42**, 39 (2009).
3. R. Bashyam, P. Zelenay, *Nature*, **443**, 63 (2006).
4. Y. J. Feng, T. He, N. Alonso-Vante, *Chem Mater*, **20**, 26 (2008).
5. M.Y. Wang, J.H. Chen, Z. Fan, H. Tang, G.H. Deng, D.L. He, et al., *Carbon*, **42**, 3257 (2004).
6. H. Tang, J.H. Chen, Z.P. Huang, D.Z. Wang, Z.F. Ren, L.H. Nie, et al., *Carbon*, **42**, 191 (2004).
7. S. Maldonado, K. J. Stevenson, *J. Phys. Chem. B*, **109**, 4707 (2005).
8. P. H. Matter, E. Wang, M. Arias, E. J. Biddinger, U. S. Ozkan, *J. Mol. Catal. a-Chem.*, **264**, 73 (2007).
9. P. H. Matter, E. Wang, M. Arias, E. J. Biddinger, U. S. Ozkan, *J. Phys. Chem. B*, **110**, 18374 (2006).
10. K. P. Gong, F. Du, Z. H. Xia, M. Durstock, L. M. Dai, *Science*, **323**, 760 (2009).
11. M. Lefevre, J. P. Dodelet, P. Bertrand, *J. Phys. Chem. B*, **106**, 8705 (2002).
12. J. B. Yang, D. J. Liu, N. N. Kariuki, L. X. Chen, *Chem. Commun.*, 329 (2008).
13. S. Maldonado, K. J. Stevenson, *J. Phys. Chem. B*, **108**, 11375 (2004).
14. M. Terrones, H. Terrones, N. Grobert, W. K. Hsu, Y. Q. Zhu, J. P. Hare, et al., *Appl. Phys. Lett.*, **75**, 3932 (1999).
15. M. Terrones, P. Redlich, N. Grobert, S. Trasobares, W. K. Hsu, H. Terrones, et al., *Adv. Mater.*, **11**, 655 (1999).
16. B. G. Sumpter, V. Meunier, J. M. Romo-Herrera, E. Cruz-Silva, D. A. Cullen, H. Terrones, et al., *Acs Nano*, **1**, 369 (2007).
17. J. W. Jang, C. E. Lee, S. C. Lyu, T. J. Lee, C. J. Lee, *Appl. Phys. Lett.*, **84**, 2877 (2004).
18. B. G. Sumpter, J. S. Huang, V. Meunier, J. M. Romo-Herrera, E. Cruz-Silva, H. Terrones, M. Terrones, *Int. J. Quantum. Chem.*, **109**, 97 (2009).
19. J. Liu, R. Czerw, D. L. Carroll, *J. Mater. Res.*, **20**, 538 (2005).
20. P. H. Matter, L. Zhang, U. S. Ozkan, *J. Catal.*, **239**, 83 (2006).
21. S. Maldonado, S. Morin, K. J. Stevenson, *Carbon*, **44**, 1429 (2006).